Desalination and Water Treatment
www.deswater.com
doi: 10.5004/dwt.2021.27874

243 (2021) 107–115
December

Determination of the effectiveness of commercial polymeric membranes for carbon dioxide separation

Grzegorz Wiciak[a,*], Aleksandra Janusz-Cygan[b], Katarzyna Janusz-Szymańska[a], Marek Tańczyk[b]

[a]*Department of Power Engineering and Turbomachinery, Silesian University of Technology, Gliwice, Poland, email: grzegorz.wiciak@polsl.pl (G. Wiciak)*
[b]*Institute of Chemical Engineering, Polish Academy of Sciences, Gliwice, Poland*

Received 29 May 2021; Accepted 31 August 2021

ABSTRACT

This paper presents both experimental results and model calculations concerning polymer membranes used for carbon dioxide separation. Experiments on a laboratory stand provided a reference for the modeling process and were then used to verify the results obtained from computational simulations. In the analyses, a 2-component gas mixture consisting of CO_2 and N_2 and a 3-component mixture containing additionally oxygen were used. Experimental work was conducted for commercial modules for air separation. Dimensionless parameters of the membrane module model such as pressure ratio, permeation number, ideal selectivity coefficients were used and determined in the model computations. The experimental results obtained for one of the studied modules were adapted for the other membrane module, differing in membrane surface area. The investigations allowed us to determine the effectiveness of a commercial polymeric membrane designed for air separation in the carbon dioxide removal process.

Keywords: Membrane module; Gas separation; UBE polymeric membranes

1. Introduction

Membrane gas separation is based on exploiting the differences in solubility and diffusivity of different gases in the specific polymers that make up the membrane. It is a process in which the driving force is the difference in partial pressures of the removed pollutants on both sides of the membrane [1–3]. By selecting appropriate types of polymeric membranes (research is in progress to find materials) it is possible to separate virtually any mixture of gaseous components. In this area membrane technologies are replacing well-known processes such as absorption, adsorption, or cryogenics [4–6]. Currently, membrane technologies for gas separation are most widely used in the following applications: enrichment of biogas with methane, denitrification of natural gas, enrichment of air with nitrogen, enrichment of air with oxygen, fractionation of hydrocarbons from natural gas, dewatering of gas streams [7–15].

The development of membrane technologies is currently very dynamic. The dynamics of this development are evidenced by the examples of many scientific publications [16–19] and advertised technological solutions. However, a certain regularity can be observed in scientific publications, which is closely related to the fact that several hundreds of membrane materials are being described, most of the currently applied industrial solutions are based on less than ten polymers, which have been known for a long time [20,21].

Indeed materials with better separation properties have already been synthesized and studied, but these materials

* Corresponding author.

have not yet achieved commercial success. A new membrane still has to meet many conditions from development to full implementation of a commercial product with industrial value, and this requires research and time. In addition to high separation capacity, the material must also be robust and, just as importantly, cost-effective. On the other hand, commercial membranes manufactured today have better selectivity and permeability than those created at the dawn of this technology [22,23]. In addition, the technologies in question are under continuous development and there is no doubt that their use will continue to grow.

Membrane installations for biofuel dehydration and separation of gaseous mixtures of organic compounds are currently at the initial stage of implementation. Materials with very promising separation properties, including new polymeric materials, metal-organic networks, and graphene membranes, are in the research phase [21–27].

Due to the high demand for new processes for the separation of gaseous mixtures, the application of mature membrane materials is sought. However, designing such processes, conducting simulation computations, cost and parametric optimization require the availability of fundamental data such as membrane permeability to the components of the mixture to be separated and membrane thickness and surface area. For research tests conducted using commercial modules, these parameters, especially the last two, are usually not available and are covered by trade secrets. Attempting to determine these quantities independently leads to the destruction of the membrane module. On the other hand, from the point of view of modeling the separation process being analyzed and/or scaling up, the product of the permeance and the membrane area may be the parameter used.

This paper presents a method for evaluating the separation efficiency of commercial membranes in a new gas separation process under development and for the acquisition of the data necessary for its design. Using the example of the process of carbon dioxide separation from CO_2/N_2 and $CO_2/N_2/O_2$ mixtures in commercial modules [2,5,6,28–31], the results of comprehensive experimental and theoretical studies leading to the determination of the permeation of mixture components and the verification of the mathematical model as a tool for process design are discussed. These studies, which used UBE modules UMS-A2 and UMS-A5, from one series, designed for air separation, included: determination of permeance of pure mixture components in UMS-A5 module, experimental studies of mixture separation for different process parameters in both modules, determination of membrane surface area in modules, and development and verification of membrane model.

2. Test methodology

2.1. Membrane modules

Two hollow fiber modules were used for this study: UMS-A2 and UMS-A5, supplied by UBE. The modules, mainly designed for air separation, used a polyimide membrane. The parameters used in the experiments were within the pressure and temperature ranges recommended by the manufacturers. The suppliers did not disclose data on membrane area and thickness. The technical parameters of the modules are shown in Table 1 [2,32].

2.2. Measuring systems and feed gases

Research on gas separation processes was conducted on two different laboratory stands (research was conducted at two independent research centers). At one of the stands, the UMS-A2 module was used, while at the other stand the tests were conducted using the UMS-A5 module. The conditions and measurement parameters for both installations were identical or similar in many tests; any differences between the parameters did not affect the comparative results. Therefore, it was possible to make a comparative analysis of the experimental results from both measurement installations.

A generalized scheme of the measurement installation for comparative tests is shown in Fig. 1 [2,6,28,29]. The feed gas stream, after measuring its parameters, that is, composition, pressure, temperature, and flow rate, is directed to the membrane module, where it is separated into two streams: the stream permeating the membrane and the stream stopped on the membrane. On the receiving line of both gas streams, we have controlled their main parameters, that is, flow rate, gas composition, and pressure. In such a plant the parameters of the separation process of both pure gases and their mixtures were determined.

It was assumed that both membrane modules belong to the same series, so the membrane is made of the same modified polyimide and has the same thickness. The same diameter of the modules allows us to assume the same number of fibers. The tested modules differ only in length. Therefore, for the simulation calculations of the UMS-A2 module, the (AQ')'s (AQ' – the product of membrane area and permeance) obtained for the UMS-A5 module were used, which were proportionally reduced by the amount related to the lengths of the working parts of the individual modules. These results are presented later in this paper.

The maximum content of CO_2 in power exhaust gases depends on the type of fuel [33,34] and for hard coal is: 18.6%–19.2% CO_2 max., for lignite 8.7%–19.5% CO_2 max., for heavy oil (mazut) 15.5% CO_2 max., for light oil: 15.3%–15.4% CO_2 max., and for natural gas: 9.5%–12.5% (15)% CO_2 max. Therefore, in the UBE UMS-A2 study, the membrane module was fed with two-component mixtures with compositions: 20% CO_2, 80% N_2, followed by 50% CO_2, 50% N_2, and three-component mixtures with the compositions: 15% CO_2, 81% N_2, 4% O_2; 15% CO_2, 70% N_2, 15% O_2; and 57% CO_2, 20% N_2, 23% O_2. In contrast, in the UBE UMS-A5 study, the membrane module was fed with two-component mixtures with the compositions: 40% CO_2, 60% N_2; 70% CO_2, 30% N_2, and three-component mixtures with the compositions: 70% CO_2, 28% N_2, 2% O_2 and 70% CO_2, 25% N_2, 5% O_2 (synthetic exhaust gas after first-stage concentration, for example, in a hybrid system). For the UMS-A2 module, laboratory-prepared standard gas mixtures in cylinders were used. For UMS-A5, we used gas mixtures prepared in a gas mixer from standard gases. The concentration of the mixture components was measured in three gas streams with an accuracy of

Table 1
Comparison of modules

Module type	UMS-A2	UMS-A5
Manufacturer	UBE	UBE
Housing material	Stainless steel	Stainless steel
Membrane material	Modified polyimide	Modified polyimide
Length, mm	430	680
Length of the working part of the module, mm	213	465
Diameter of the wider part of the module/diameter of the working part, mm/mm	47/29*	47/29*
Weight, kg	1.9	2.2
Maximum inlet temperature, °C	40	40
Maximum inlet pressure, bar(g)	9.9	9.9
Maximum particle size in the feed gas, μm	0.01	0.01
Maximum oil content in the feed gas, ppm	0.001	0.001

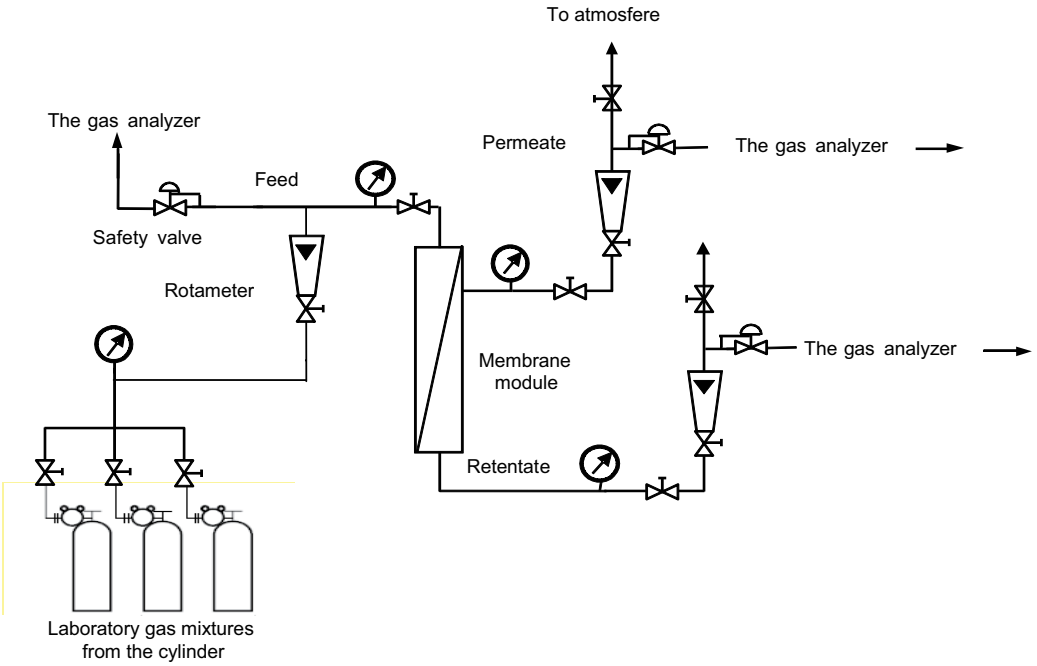

Fig. 1. Generalized schematic diagram of the installation for comparative study of CO_2 separation parameters [2,6,28,29].

0.01 vol.%. Flow meters with an accuracy of 0.1 l/min were used to measure the feed gas, retentate, and permeate flow rates. The pressure was measured with an accuracy of 0.01 bar. The temperature measurement was used, which provided an accuracy of 0.1°C.

2.3. Methodology for evaluating the effectiveness of the separation process

The most important parameters that describe the efficiency of a separation process are selectivity and permeability. Permeability determines how much of a component will pass through a membrane, while selectivity determines which components will pass through a membrane better or worse [1,2,30,35]. The feed is defined as the feed flow to the membrane, which is then separated into two streams: permeate (the flow that penetrates the membrane) and retentate (the flow that is retained by the membrane).

Most often, two quantities are used to evaluate the efficiency of the CO_2 separation process from exhaust gases. The first one is the molar or volume fraction of CO_2 in the permeate ($y_{CO_2\omega}$), which determines the purity of the permeate; the second one is the CO_2 recovery (η) which indicates what portion of CO_2 from the exhaust gas is contained in the separated stream and is expressed by the formula:

$$\eta = \frac{\left(F\, y_{CO_2}\right)_{\omega}}{\left(F\, x_{CO_2}\right)_{\alpha}} 100\% \tag{1}$$

A recovery of η = 1 means that all carbon dioxide has been separated from the exhaust gas. It is stated that the molar fraction of CO_2 in the permeate ($y_{CO_2\omega}$) and the CO_2 recovery rate should not reach values below 0.9 or even 0.95. The higher these values are the lower the carbon dioxide pollution of the atmosphere [2,10].

The permeability P_i' of a given component "i" through membranes is described as the product of sorption coefficient S_i and diffusion coefficient D_i:

$$D_i \cdot S_i = P_i' \tag{2}$$

The classical equation of gas transport (Fick's equation) through a solid membrane – the fundamental equation of the solubility-diffusion model that describes the transport of a single component and through a compact membrane [2,10] is as follows:

$$J_i = -D_i \frac{dc_i}{dx} \tag{3}$$

where J_i is the gas flow through the membrane, mol/s; c_i is the concentration of the "i'' – ingredient that permeates the membrane; x is the membrane thickness, μm.

The integral of Eq. (3) after the membrane thickness, adopting some simplifications and taking into account the design features of the capillary membrane under study and the membrane modules [2,10] results in the relationship:

$$J_i = \frac{AP_i'}{x}\left(p_{i\alpha} - p_{i\omega}\right) \tag{4}$$

From Eqs. (3) and (4) for the two gas components (CO_2 and N_2), an equation describing the ratio of elementary flows permeating the membrane can be obtained. The ideal selectivity coefficient α* is proportional to the ratio of pure gas permeability P'_{CO_2} and P'_{N_2} is expressed by the formula:

$$\alpha^* = \frac{P'_{CO_2}}{P'_{N_2}} \tag{5}$$

It is often difficult or impossible to determine the elemental flows that permeate a membrane. This is usually the case with commercial membrane modules, whose manufacturers are reluctant to disclose details of the materials used and their properties, which is also the case here.

Therefore, an important aspect is to determine the actual selectivity coefficient α, expressed as the ratio of the shares of individual components in the permeate to their shares in the feed, which was also done in this work using Eq. (6):

$$\alpha = \frac{\left(\frac{y_{CO_2}}{y_{N_2}}\right)_\omega}{\left(\frac{x_{CO_2}}{x_{N_2}}\right)_\alpha} \tag{6}$$

The efficiency of the separation process was evaluated by comparing both the product purity, that is, the molar fraction of CO_2 in the separated stream ($y_{CO_2\omega}$), and the CO_2 recovery rate coefficient (η) for both membrane modules tested, as illustrated graphically later in this paper.

The values of process parameters were determined by direct measurements of temperature, flow rates, and concentrations (volume proportions) of gases supplied to and removed from the membrane. The measurements consisted in establishing a constant flow rate of the feed using a gas regulator and control valves placed in the feed and retentate process lines (Fig. 1), and for constant pressure, after the process had stabilized, process parameters were recorded. During the measurements, minimal fluctuations of the flow rates were observed (recorded) at the level of about ±1%, which resulted, among other things, from the accuracy of the applied measuring devices and the manual control method.

2.4. Methodology of numerical comparative tests

Mathematical modeling has become an essential tool in the design process, as the availability of reliable mathematical models eliminates the need for time-consuming and expensive experimental studies. To verify the transferability of experimentally determined permeation coefficients from one module to another module but belonging to the same series, simulation calculations were carried out for the UMS-A2 module using the permeation coefficients obtained for the UMS-A5 module. Considering the flow pattern of this membrane unit, plug flow is assumed on the feed side and locally unhindered flow (locally undisturbed, free-flowing permeate) on the permeate side. It is also assumed that there are no interactions between permeating components (therefore permeances are the same as for pure components), pressure drop and axial dispersion are negligible on both sides of the membrane, the process is isothermal, and concentration polarization is negligible on both sides of the membrane. The gas flow scheme in the membrane module and the model equations along with the boundary conditions are given in [5]. The model was implemented in the gPROMS modeling environment (PSE, UK). The model consists of ordinary and algebraic differential equations, and the fourth-order finite difference method (CFDM) with 100 discretization intervals was used to discretize the axial domain. The resulting system of algebraic equations was solved using the general DASOLV code. The computations were performed on a desktop workstation equipped with two 14-core 2.4 GHz INTEL Xeon processors and 128 GB of RAM. A schematic of the solution procedure is shown in Fig. 2a and the gas flow distribution in the membrane module is shown in Fig. 2b.

We input data into the model (additionally, new designations are introduced) such as flow rate (F_α), composition ($x_{i\alpha}$) and pressure of the feed gas (p_α), pressure on the permeate side (p_ω), and the product of membrane area and permeance of each component of the input mixture (AQ_i'). The dimensionless model parameters such as pressure ratio (δ), permeation number (R), and ideal selectivity coefficient (α*) are then calculated. The calculations result in the following output parameters: flow rate and composition of

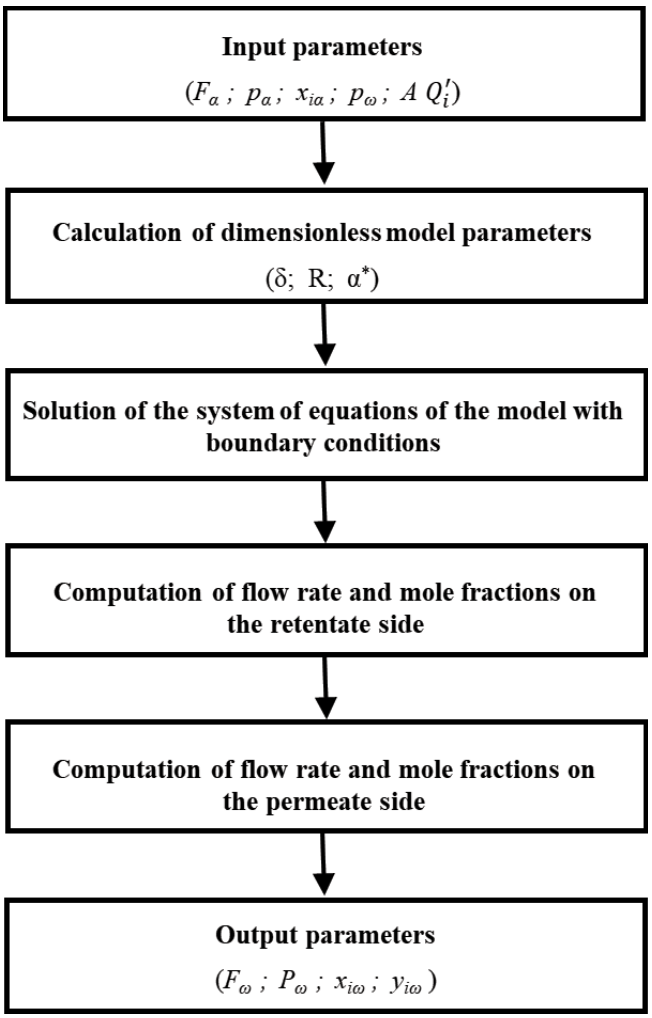

Fig. 2. (a) Solution procedure and (b) gaseous streams in a membrane module for the plug flow on the feed side and unhindered flow on the permeate side [5].

both permeate (P_ω, $y_{i\omega}$) and retentate (F_ω, $x_{i\omega}$). The equations used in the model are presented in the following section.

Mathematical model equations and boundary conditions [5].

Local mole fraction of component 1 on the permeate side:

$$y_1^+ \sum_{i=1}^{N} \frac{\alpha_{i1} x_i}{x_1 - \delta y_1^+ \left(1 - \alpha_{i1}\right)} - 1 = 0 \tag{7}$$

Local mole fractions of the other permeate components ($i = 2, \ldots, N$):

$$y_i^+ = \frac{\alpha_{i1} x_i y_1^+}{x_1 - \delta y_1^+ \left(1 - \alpha_{i1}\right)} \tag{8}$$

Gas composition on the feed side ($i = 1, \ldots, N–1$):

$$\frac{dx_i}{dz} = -R \frac{y_1 - x_1}{y_1 - x_{1\alpha}} \left[\alpha_{i1} \left(x_i - \delta y_i^+ \right) - x_i \sum_{j=1}^{N} \alpha_{j1} \left(x_j - \delta y_j^+ \right) \right] \tag{9}$$

Mole fraction of component N on the feed side:

$$x_N = 1 - \sum_{i=1}^{N-1} x_i \tag{10}$$

Mole fraction of component 1 in the permeate:

$$\frac{dy_1}{dz} = R \frac{y_1 - x_1}{x_{1\alpha} - x_1} \left[\left(x_1 - \delta y_1^+ \right) - y_1 \sum_{j=1}^{N} \alpha_{j1} \left(x_j - \delta y_j^+ \right) \right] \tag{11}$$

Mole fractions of the other permeate components ($i = 2, \ldots, N–1$):

$$y_i = \frac{x_i \left(y_1 - x_{1\alpha} \right) - x_{i\alpha} \left(y_1 - x_1 \right)}{x_1 - x_{1\alpha}} \tag{12}$$

Mole fraction of component N on the permeate side:

$$y_N = 1 - \sum_{i=1}^{N-1} y_i \tag{13}$$

Boundary conditions at $z = 0$ ($i = 1, \ldots, N$):

$$x_i = x_{i\alpha} \tag{14}$$

$$y_i = y_{i\alpha}^+ \tag{15}$$

Retentate flow rate:

$$F_\omega = F_\alpha \frac{y_{1\omega} - x_{1\alpha}}{y_{1\omega} - x_{1\omega}} \tag{16}$$

Permeate flow rate:

$$P_\omega = F_\alpha - F_\omega \tag{17}$$

3. Experimental results and simulation calculations

3.1. The pure gases

Permeation research of pure gases (CO_2, O_2, N_2) was performed in an experimental installation, the detailed description of which is presented by the study of Janusz-Cygan et al. [29]. A polymeric membrane module of UBE type UMS-A5 was used in the research. The flow rate, pressure, and temperature in the feed flow, retentate and permeate were measured and controlled during the pure gas permeation tests. For each pure component and temperature, the average values of the product of permeance and module area were determined (for pure gases the product of permeation and the area of the module (AQ′) was determined), which was called module permeance [29].

Based on the data of Li et al. [36], the methodology presented by the study of Kotowicz et al. [2], and the ideal CO_2/N_2 and CO_2/O_2 selectivity coefficients obtained in the UMS-A5 module [29], it was estimated that the effective working area for the UMS-A2 module is 76 cm^2 and for the

UMS-A5 module is 167 cm². On this basis, the average permeance values of carbon dioxide, nitrogen, and oxygen in the membrane material (polyimide) were determined for three gas temperatures.

Li et al. [36], it is reported that the CO_2 permeance for new "cardo-type polyimide" membranes is Q'_{CO_2} = 1.3 × 10⁻³ cm³(STP)/(cm² s cm Hg) and CO_2/N_2 = 41 for 298 K. Kotowicz et al. [2], the methodology to obtain the CO_2 permeance for the UMS-A2 module was presented and it was Q'_{CO_2} = 3.8413 m^3_u/(m² h bar). Comparing the two coefficients (reducing to common units) gives the same value, so we know the Q'_{CO_2}. We assume that the membranes in UMS-A2 and UMS-A5 modules are made of the same polymer. This is confirmed by the value of CO_2/N_2 selectivity coefficient = 45 (close to 41 – literature) obtained for UMS-A5 at 298 K. Knowing the product of permeance and membrane area $(AQ')_{CO_2}$ determined for pure gas in UMS – A5 module Janusz-Cygan et al. [29] and Q'_{CO_2} [2,36] we determine the area of the UMS-A5 module. Using the conversion factor associated with the length of the working parts of the studied modules, we also determine the surface area of the UMS-A2 module.

It can be observed that the best permeating gas through this membrane is carbon dioxide and the least permeating is nitrogen. The ideal CO_2/N_2 selectivity coefficient is 50.3 at a temperature equal to 288 K. A 10 K increase in temperature results in a decrease in CO_2/N_2 of about 10%. The permeance values from Table 2 were used in the simulation calculations for both the UMS-A5 and UMS-A2 modules.

3.2. Two-component mixture

The separation results of gas mixtures containing 40 or 70 vol.% CO_2 in N_2, for a feed gas flow rate of 900 L/h and a temperature of 295 K is shown in Fig. 3. Although these data were already presented by the study of Janusz-Cygan et al. [29], they are presented again for better clarity of the article.

From the figure shown, it can be seen that nearly 99 vol.% CO_2 purity can be achieved in the UMS-A5 membrane module for a feed mixture containing 70 vol.% CO_2. On the other hand, more than 94 vol.% CO_2 purity can be achieved for a feed mixture containing 40 vol.% CO_2. It is important to note that the concentration of carbon dioxide in the permeate is virtually constant, independent of the pressure ratio. CO_2 recovery, on the other hand, strongly depends on the pressure ratio; as the pressure ratio increases, the CO_2 recovery efficiency increases. Thus, for a feed mixture containing 70 vol.% CO_2 and a pressure ratio of 7, we obtain 98.6 vol.% CO_2 in the permeate at 28% efficiency of CO_2 recovery. The figure also shows very good agreement between experimental results and numerical simulations.

Gas permeation research for the UBE UMS-A2 module is presented in detail in the paper [2,6,28,30,31], where a description of the installation and measurement system is also included. The results of membrane separation tests for mixtures containing 20 or 50 vol.% CO_2 in N_2 are shown in Figs. 4 and 5. In this case, the ratio of feed pressure to permeate pressure was constant and was about 7, while the flow rates of the feed gas were changed.

From the presented figures, it can be seen that the CO_2 concentration in the permeate initially increases and then stabilizes at: 75 vol.% for a feed mixture containing

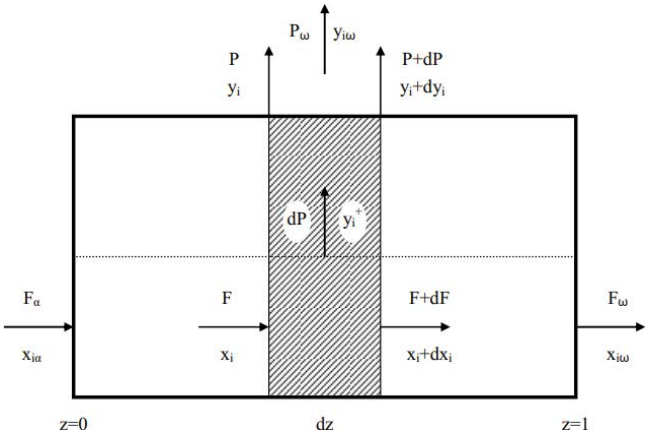

Fig. 3. The efficiency of the separation process for mixtures containing 40 and 70 vol.% CO_2 in N_2; (symbols – experiments; lines – computations).

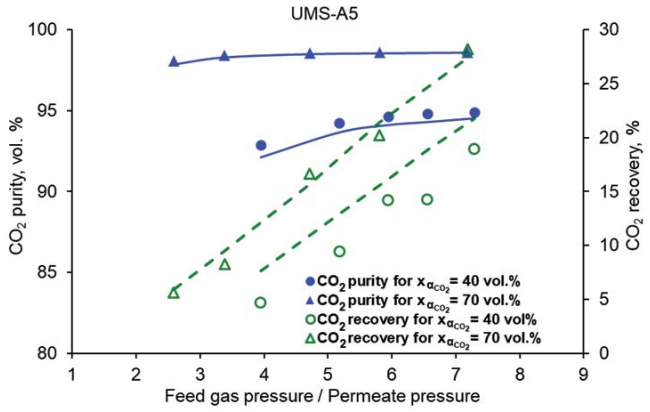

Fig. 4. The efficiency of the separation process for a mixture containing 20 vol.% CO_2 in N_2; (symbols – experiments; lines – computations).

Table 2
The permeance of carbon dioxide, nitrogen, and oxygen in UBE UMS-A5 and UMS-A2

Q', GPU	Feed pressure, bar(a)	288 K	293 K	298 K
CO_2	1.8–7.5	1,174 ± 132	1,222 ± 120	1,299 ± 96
O_2	2.0–7.5	210 ± 6.0	228 ± 6.0	269 ± 6.0
N_2	3.0–7.5	23.4 ± 0.6	26.3 ± 1.2	28.7 ± 0.6

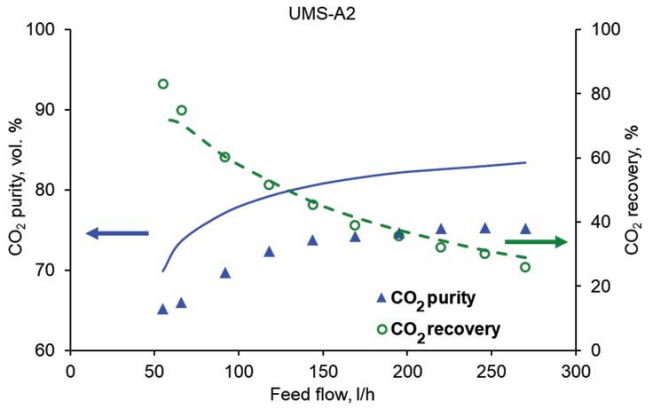

Fig. 5. The efficiency of the separation process for a mixture containing 50 vol.% CO_2 in N_2; (symbols – experiments; lines – computations).

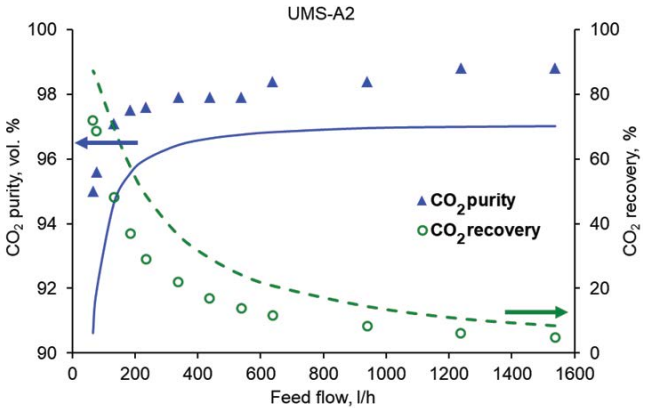

Fig. 6. The efficiency of the separation process for mixtures containing CO_2, N_2, and O_2; (symbols – experiments; lines – computations).

20 vol.% CO_2 and almost 99 vol.% for a feed mixture containing 50 vol.% CO_2. The carbon dioxide recovery efficiency decreases as the feed gas flow rate increases. For example, for a mixture containing 50 vol.% CO_2 and for a flow rate of 185 l/h, a 97.5 vol.% purity of CO_2 was obtained with an almost 37% recovery rate of the desired component. In the case of gas permeation processes, the efficiency of the separation process is determined by both the purity of the product and its recovery efficiency. Therefore, for the UMS-A2 module, the most efficient separation process is for feed gas flow rates in the range of 50–100 L/h for a feed mixture containing 20 vol.% CO_2, and from 100–300 L/h for a feed mixture containing 50 vol.% CO_2.

It is also interesting to notice that good compatibility between experimental tests and numerical simulations was obtained, although the calculations were performed using data obtained for another membrane module located in the same series of this company.

3.3. Three-component mixture

Separation experiments for three-component mixtures were performed in both the UMS-A2 and UMS-A5 modules. In the UMS-A5 module, tests were conducted for mixtures containing 70 vol.% CO_2, oxygen with a concentration in the range of 0–5 vol.%, and nitrogen. The feed gas flow rate was 900 l/h and the feed gas pressure was varied in the range of 1.2–7.5 bar(a) using a gas regulator. The obtained results are shown in the graphic form in Fig. 6.

The figure shows that the presence of oxygen in the feed mixture has little effect on the purity of the permeate. An increase in the concentration of oxygen in the feed mixture limits from 0 to 5 vol.% resulted in a decrease in the CO_2 concentration in the permeate by 1.3 percentage points. Furthermore, it can be concluded that the addition of O_2 in the feed mixture has virtually no effect on CO_2 recovery efficiency.

The UMS-A2 module was tested for mixtures containing 15 vol.% CO_2, oxygen with a concentration in the range of 4–15 vol.%, and nitrogen. The feed gas pressure was 6 bar(a) and the feed gas flow rate was varied in the range of 60–1,600 L/h. The results obtained are shown in Figs. 7 and 8.

Also for three-component mixtures, a similar pattern of curves as for two-component mixtures was obtained. Thus, an increase in the feed gas flow rate causes, after an initial increase in CO_2 purity, some stabilization, with a decrease in CO_2 recovery efficiency. These figures also show very good compatibility between experimental results and numerical simulations. Therefore, it can be concluded that the proposed solution, that is, the use of modified module permeances obtained for one module can be applied to numerical computations of another module, but belonging to the same series of types. Confirmation of this hypothesis is perfectly seen in Fig. 9, where both studied modules are shown in one figure. Because the average relative error between experimental results and numerical simulations for CO_2 purity is for the UMS-A5 module, 0.28%, for the UMS-A2 module only 2.4% for the three-component mixture, it can be concluded that the same type of membrane was used in both compared modules.

4. Summary

In the presented work, the applicability of two commercial UBE modules (UMS-A2 and UMS-A5) designed for air separation, in the process of CO_2 separation from two and three-component mixtures with nitrogen and oxygen, was positively verified. Based on experimental and theoretical research conducted independently in two laboratories, the membrane area in both modules was estimated and the permeance of carbon dioxide, nitrogen, and oxygen in the membrane material (polyimide) was determined for three gas temperatures. A model with the plug flow on the feed side and unhindered flow on the permeate side was used for the mathematical description of the mixture separation. The model, as a tool for process design and scale transfer, has been comprehensively verified for a wide range of operating parameters (pressure, composition, and flow rate of the feed mixture) based on the results of experimental research on mixture separation.

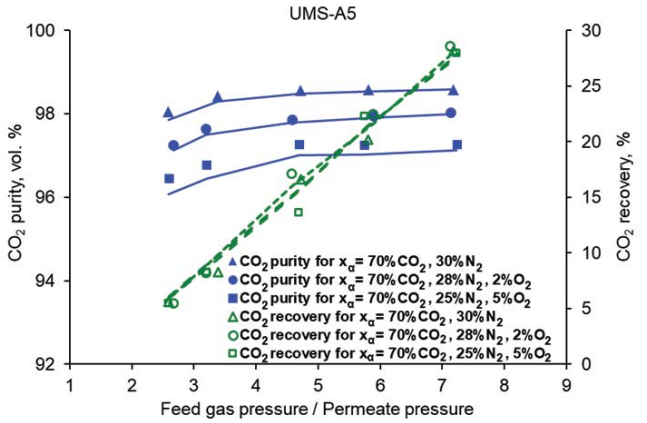

Fig. 7. The efficiency of the separation process for a mixture containing 15 vol.% CO_2, 81 vol.% N_2, 4 vol.% O_2; (symbols – experiments; lines – computations).

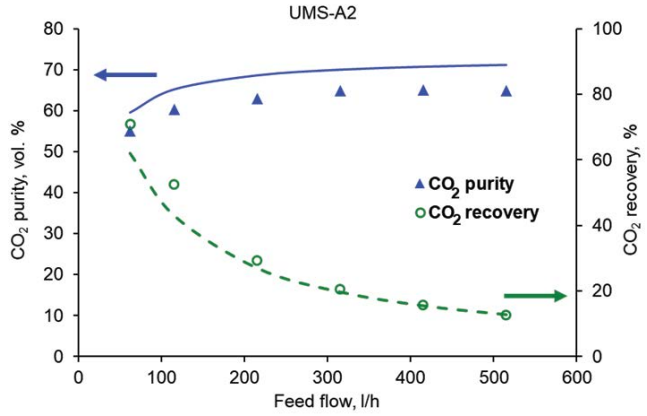

Fig. 8. The efficiency of the separation process for a mixture containing 15 vol.% CO_2, 70 vol.% N_2, 15 vol.% O_2; (symbols – experiments; lines – computations).

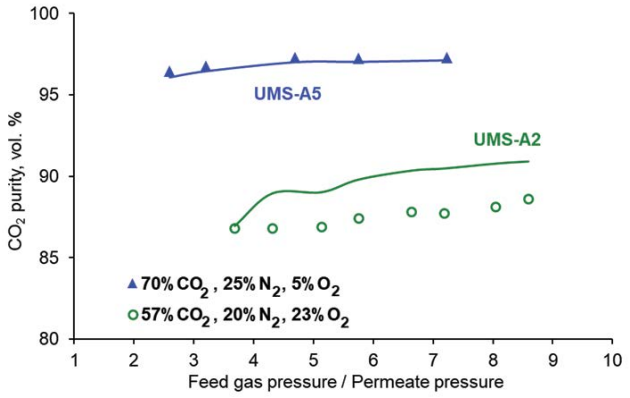

Fig. 9. Separation of ternary mixtures in UMS-A2 and UMS-A5 modules; (symbols – experiments; lines – computations).

Symbols

A	—	Membrane area, m^2
AQ′	—	Product of membrane area and permeance (constant for a given membrane module and a given gas)
c_i	—	Concentration of the "i" – ingredient that permeates the membrane
D	—	Diffusion coefficient, m^2/s
F_α	—	Feed flow rate on the module inlet, kmol/h or mol/s
F_ω	—	Retentate flow rate, kmol/h or mol/s
J	—	Gas flow through the membrane, mol/s
L_{MB}	—	Membrane module length, m
N	—	Number of components
P_ω	—	Permeate flow rate, kmol/h or mol/s
P'	—	Permeability, mol/(m s Pa)
P'_1	—	Permeability to reference components – it is the permeability of the fastest permeating Component
p_α	—	Pressure on the module inlet, bar or Pa
p_ω	—	Pressure on the permeate side, bar or Pa
Q'	—	Permeance (=P'/x), mol/(m^2 s Pa) or kmol/(m^2 h bar)
R	—	Permeation number (=AQ′$_1 p_\alpha/F_\alpha$)
S	—	Sorption coefficient, mol/(m^3 Pa)
x	—	Membrane thickness, μm or m
x_α	—	Mole fraction on the feed side
x_ω	—	Mole fraction on the retentate side
y^+	—	Local mole fraction of the permeate side
y, y_ω	—	Mole fraction on the permeate side
Z	—	Linear coordinate in the membrane model, m
z	—	Dimensionless module length coordinate in the membrane module (=Z/L_{MB})
α*	—	Ideal selectivity coefficient (=P'/P'_1)
α	—	Actual selectivity coefficient
δ	—	Pressure ratio (=p_ω/p_α)
η	—	CO_2 recovery, %

Subscripts and superscripts

N	—	Number of components
α	—	Module inlet
ω	—	Module outlet
i, j	—	Component "i", "j"
1	—	Reference component (component with the highest permeability)
+	—	Local values

Acknowledgments

The research has been financially supported by the Silesian University of Technology by statutory research funds within the framework of project no.: 08/050/BK_21/0231.

References

[1] M. Bodzek, J. Bohdziewicz, K. Konieczny, Techniki membranowe w ochronie środowiska, Wydawnictwo Politechniki Śląskiej, Gliwice, 1997.
[2] J. Kotowicz, K. Janusz-Szymańska, G. Wiciak, Technologie membranowe wychwytu dwutlenku węgla ze spalin dla

nadkrytycznego bloku węglowego, Wydawnictwo Politechniki Śląskiej, Monografia – Politechnika Śląska, Gliwice, 2015.
[3] E. Biernacka, T. Suchecka, Techniki membranowe w ochronie środowiska, Wydawnictwo SGGW, Warszawa, 2004.
[4] S. Yan, M. Fang, W. Zhang, W. Zhong, Z. Luo, K. Cen, Comparative analysis of CO_2 separation from flue gas by membrane gas absorption technology and chemical absorption technology in China, Energy Convers. Manage., 49 (2008) 3188–3197.
[5] M. Jaschik, M. Tanczyk, J. Jaschik, A. Janusz-Cygan, The performance of a hybrid VSA-membrane process for the capture of CO_2 from flue gas, Int. J. Greenhouse Gas Control, 97 (2020) 103037, doi: 10.1016/j.ijggc.2020.103037.
[6] G. Wiciak, L. Remiorz, J. Kotowicz, Instalacja laboratoryjna do synchronicznych badań separacji ditlenku węgla metodami membranową i akustyczną. Analiza systemów energetycznych. Praca zbiorowa. Pod red. B. Węglowskiego, P. Dudy. Kraków: Wydaw. Politechniki Krakowskiej, 2013, pp. 331–349.
[7] J.J. Marano, J.P. Ciferino, Integration of gas separation membranes with IGCC identifying the right membrane for the right job, Energy Procedia, 1 (2008) 361–368.
[8] M. Harasimowicz, P. Orluk, G. Zakrzewska-Trznadel, A.G. Chmielewski, Application of polyimide membranes for biogas purification and enrichment, J. Hazard. Mater., 144 (2007) 698–702.
[9] R. Abdulrahman, I. Sebastine, Natural gas dehydration process simulation and optimization: a case study of Khurmala Field in Iraqi Kurdistan Region, World Acad. Sci. Eng. Technol., 78 (2013) 469–472.
[10] K. Janusz-Szymańska, A. Dryjańska, Possibilities for improving the thermodynamic and economic characteristics of an oxy-type power plant with a cryogenic air separation unit, Energy, 85 (2015) 45–61.
[11] T.-S. Chung, L. Ying Jiang, Y. Li, S. Kulprathipanja, Mixed matrix membranes (MMMs) comprising organic polymers with dispersed inorganic fillers for gas separation, Progr. Polym. Sci., 32 (2007) 483–507.
[12] H. Feng, H. Zhang, L. Xu, Polymeric membranes for natural gas conditioning, Energy Sources Part A, 29 (2007) 1269–1278.
[13] C.V. Funk, D.R. Lloyd, Zeolite-filled microporous mixed matrix (ZeoTIPS) membranes: prediction of gas separation performance, J. Membr. Sci., 313 (2008) 224–231.
[14] D. Bergmair, S.J. Metz, H.C. de Lange, A.A. van Steenhoven, System analysis of membrane facilitated water generation from air humidity, Desalination, 339 (2014) 26–33.
[15] J.R. Pauls, D. Fritsch, T. Klassen, K.-V. Peinemann, Gas permeation measurement under defined humidity via constant volume/variable pressure method, J. Membr. Sci., 389 (2012) 343–348.
[16] K.-J. Huang, S.-J. Hwang, W.-H.L. Lai, The influence of humidification and temperature differences between inlet gases on water transport through the membrane of a proton exchange membrane fuel cell, J. Power Sources, 284 (2015) 77–85.
[17] C.Y. Chuah, J. Lee, J. Song, T.-H. Bae, Carbon molecular sieve membranes comprising graphene oxides and porous carbon for CO_2/N_2 separation, Membranes, 11 (2021) 284, doi: 10.3390/membranes11040284.
[18] Z. Tong, A.K. Sekizkardes, Recent developments in high-performance membranes for CO_2 separation. Membranes, 11 (2021) 156, doi: 10.3390/membranes11020156.
[19] M. Szwast, D. Polak, M. Zalewski, Novel gas separation membrane for energy industry, Desal. Water Treat., 64 (2017) 255–259.
[20] H. Sijbesma, K. Nymeijer, R. van Marwijk, R. Heijboer, J. Potreck, M. Wessling, Flue gas dehydration using polymer membranes, J. Membr. Sci., 313 (2008) 263–276.
[21] Y. Han, Y. Yang, W. S. Winston Ho, Recent progress in the engineering of polymeric membranes for CO_2 capture from flue gas, Membranes, 10 (2020) 365, doi: 10.3390/membranes10110365.
[22] Y. Wang, L. Zhao, A. Otto, M. Robinius, D. Stolten, A review of post-combustion CO_2 capture technologies from coal-fired power plants, Energy Procedia, 114 (2017) 650–665.
[23] P. Pandey, R.S. Chauhan, Membranes for gas separation, Progr. Polym. Sci., 26 (2001) 853–893.
[24] R. Rea, M.G. De Angelis, M.G. Baschetti, Models for facilitated transport membranes: a review, Membranes, 9 (2019) 26, doi: 10.3390/membranes9020026.
[25] J. Davidson, K. Thambimuthu, Technologies for Capture of Carbon Dioxide, Proceedings of the Seventh Greenhouse Gas Technology Conference, Vancouver, Canada, International Energy Association (IEA), Greenhouse Gas R&D Programme, 2004.
[26] L. Ansaloni, M. Minelli, M. Giacinti Baschetti, G.C. Sarti, Effect of relative humidity and temperature on gas transport in Matrimid®: experimental study and modeling, J. Membr. Sci., 471 (2014) 392–401.
[27] A. Jankowski, E. Grabiec, K. Nocoń-Szmajda, A. Marcinkowski, H. Janeczek, A. Wolińska-Grabczyk, Polyimide-based membrane materials for CO_2 separation: a comparison of segmented and aromatic (Co)polyimides, Membranes, 11 (2021) 274, doi: 10.3390/membranes11040274.
[28] G. Wiciak, K. Janusz-Szymańska, J. Kotowicz, Badania eksperymentalne i numeryczne separacji CO_2 membran polimerowych z zastosowaniem gazowej mieszanki wzorcowej, Rynek Energii, 2 (2014) 98–103.
[29] A. Janusz-Cygan, J. Jaschik, A. Wojdyła, M. Tańczyk, The separative performance of modules with polymeric membranes for a hybrid adsorptive/membrane process of CO_2 capture from flue gas, Membranes, 10 (2020) 309, doi: 10.3390/membranes10110309.
[30] G. Wiciak, K. Janusz-Szymańska, The Influence of Selected Parameters on the Real Coefficient Selectivity of the Membrane Separator Dedicated to the Separation of CO_2 from Flue Gases., Membranes and Membrane Processes in Environmental Protection, K. Konieczny, I. Korus, Eds., Monographs, Polish Academy of Sciences. Environmental Engineering Committee, Vol. 118, 2014, pp. 101–116.
[31] G. Wiciak, K. Janusz-Szymańska, L. Remiorz, The Impact of CO_2 Concentration on the Properties of a Polymer Membrane Separator Intended for the CCS Technology, 27th International Conference on Efficiency, Cost, Optimization, Simulation and Environmental Impact of Energy Systems (ECOS 2014), Turku, Finland, 15–19 June 2014, pp. 1316–1330.
[32] A. Janusz-Cygan, M. Jaschik, M. Tańczyk, K. Warmuziński, A. Wojdyła, R. Pawełczyk, Wydzielanie ditlenku węgla ze spalin energetycznych w komercyjnych modułach membranowych z włóknami pustymi, Przemysł Chemiczny, 95 (2016) 1833–1837, doi: 10.15199/62.9.35.
[33] M. Pronobis, Modernizacja kotłów energetycznych, WNT, Warszawa, 2002.
[34] M. Pronobis, S. Ciukaj, Wpływ wilgotności paliwa na punkt rosy spalin wylotowych z kotłów energetycznych spalających biomasę, Materiały IX Konferencji Naukowo Technicznej, Ochrona Środowiska w Eksploatacji Kotłów Rusztowych, Szczyrk, 2007.
[35] R.W. Baker, K. Lokhandwala, Natural gas processing with membranes: an overview, Ind. Eng. Chem. Res., 47 (2008) 2109–2121.
[36] N. Li, A. Fane, W.S. Ho, T. Matsuura, Advanced Membrane Technology and Applications, John Wiley & Sons, Inc., Hoboken, New Jersey, 2008.